Enhanced infrared photovoltaic efficiency in PbS nanocrystal/semiconducting polymer composites: 600-fold increase in maximum power output via control of the ligand barrier

S. Zhang, P. W. Cyr, S. A. McDonald, G. Konstantatos, and E. H. Sargent[a]
Department of Electrical & Computer Engineering, University of Toronto, Toronto, Ontario M5S 3G4, Canada

We report a comparison of photoconductive performance of PbS nanocrystal/polymer composite devices containing either oleic acid-capped or octylamine capped nanocrystals (NCs). The octylamine-capped NCs allow over two orders of magnitude more photocurrent under −1 V bias; they also show an infrared photovoltaic response, while devices using oleic acid-capped NCs do not. Further improvement in the photovoltaic performance of films made with octylamine-capped NCs occurs upon thermally annealing the composite layer at 220 °C for 1 h. The procedure leads to a 200-fold increase in short circuit current, a 600-fold increase in maximum power output, and an order of magnitude faster response time. © *2005 American Institute of Physics.*
[DOI: 10.1063/1.2137895]

Composites of semiconductor nanocrystals (NCs) and conjugated polymers offer promise for fabrication of large-area optoelectronic devices on flexible substrates using low-cost solution processing. Control of the organic-inorganic interfaces on the nanoscale is of critical importance in such systems. In photovoltaic devices, rapid and efficient charge separation is needed for subsequent separate transport and extraction of electrons and holes. Organic ligands passivating the surfaces of NCs endow solubility, yet these ligands are typically insulating and thus impede charge transfer between the NC and polymer.[1] While moderate success has been achieved in conjugated polymer/NC composite-based solar cells active in the visible region,[2–5] nearly one-half of the solar energy reaching the Earth's surface lies in the infrared (IR) region beyond 700 nm, and it is therefore of great interest to develop IR-sensitive devices.[6] Recently, IR photovoltaic devices based on solution-processible nanocomposites of PbS NCs in poly[2-methoxy-5-(2′-ethylhexyloxy-*p*-phenylenevinylene)] (MEH-PPV) were reported.[7] While these initial results were promising, the devices exhibited very low efficiencies, meriting further optimization.

Reports investigating the effects of annealing on polymer-based composite photovoltaics typically cite changes in the morphology of the separate phases as the cause for improved charge separation or charge mobility.[8–11] In solar cells consisting of pyridine-capped CdSe in poly(3-hexylthiophene), an increase in the external quantum efficiency by a factor of 1.3 to 6 by heating the films is reported.[12] The influence of annealing on photovoltaics made from polymer/NC composites for use in the IR region has not been explored.

We demonstrate control of the ligand barrier in MEH-PPV/PbS NC composites by exchanging the oleic acid ligands for octylamine ligands in solution prior to casting the films, and observe a large improvement in photoconductive performance. We further demonstrate control of this interface in the solid state via thermal annealing of the films, which results in up to a 200-fold improvement in short-circuit current and 600-fold increase in maximum power output, as well as a more rapid photoconductive response.

Oleic acid-capped PbS nanocrystals were synthesized using the method of Ref. 13. Octylamine-capped PbS NCs were prepared by ligand exhange as previously described.[7] The exchange procedure leads to a blueshift of the first excitonic absorption peak of the NCs due to a ligand etching phenomenon. Thus, oleic acid-capped NCs with a first-excitonic peak at 1140 nm afforded octylamine-capped NCs with a first-excitonic peak at 985 nm after the exchange process. A second set of octylamine-capped NCs was also used with a first-excitonic absorption peak at 1300 nm. The PbS NC/MEH-PPV blend layers (80 wt % NCs) in the devices were prepared via spincoating of chloroform solutions onto indium tin oxide-coated glass. Annealing of films was performed on a hotplate for 1 h in a N_2-filled glove box with <1 ppm residual O_2 and H_2O. Upper contacts (3 mm²) were then deposited by thermal evaporation to form a metal stack of 30 nm Mg/100 nm Ag/5 nm Au. The dark and photocurrents were measured using an Agilent 4155C Semiconductor Parameter Analyzer. Optical excitation was provided by a 975 nm semiconductor laser operating in continuous wave mode, with the beam enlarged to a diameter of ∼3 mm by a lens and focused on the active device area. The response time of the devices was obtaining by measuring the voltage under zero-external applied bias across a load resistor placed in series with the device. The resistance of the series load resistor was three orders of magnitude smaller than that of the device under illumination. Thermal gravimetric analysis (TGA) was performed under N_2 using a TA Instruments SDT Q600 with a heating rate of 10 °C min⁻¹. Photoluminescence spectra were obtained using the system described in Ref. 14.

Figure 1 plots the current-voltage (*I*-*V*) characteristic, with and without infrared illumination, for devices using PbS NCs as-synthesized (oleic acid ligands, first-exciton peak at 1140 nm) and following exchange (octylamine ligands, first-exciton peak at 985 nm). The data have been normalized to account for differences in absorption at the excitation wave-
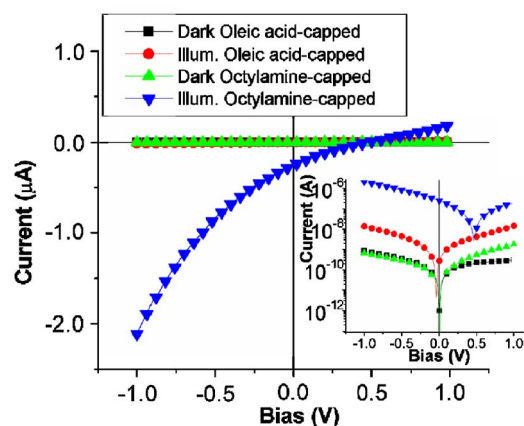
FIG. 1. (Color online) Dark and illuminated (200 mW) *I-V* curves of devices made with oleic acid-capped (squares and circles) and octylamine capped (triangles) PbS nanocrystals. Inset shows the same data in a semilog plot.

FIG. 2. (Color online) Photocurrent *I-V* curves under 200 mW illumination for an unannealed sample (squares), and samples annealed at 160 °C (circles), 190 °C (triangles), and 220 °C (stars). Inset shows same data in semilog plot.

length of the NC samples. No thermal annealing was performed on these samples. No detectable photovoltaic response is observed in the devices using oleic acid-capped NCs. In comparison, the device prepared with octylamine-capped NCs showed 160 times more photocurrent at −1 V, a short-circuit current (I_{sc}) of 250 nA and an open-circuit potential (V_{oc}) of 0.47 V.

The longer oleic acid ligands (comprising an 18 carbon chain) are ∼2 nm in length, and provide a significantly greater barrier to dissociation of the exciton created in the nanocrystal at the NC/polymer interface than the much shorter octylamine ligands (comprising an 8 carbon chain), which are ∼1 nm in length. Under zero-applied bias, the built-in field due to the contact work function offset is insufficient to lead to an appreciable charge transfer between the oleic acid-capped NC and polymer. Under applied bias, only a weak photocurrent is observed in this device. In contrast, charge separation is greatly enhanced in devices based on NCs capped using the shorter octylamine ligands, leading to significantly greater photocurrent generation. This could be due to either more efficient tunneling through the ligand barrier, or direct transfer to polymer at bare sites on the NC surface present after the ligand exchange process. Consistent with this, a reduction in interparticle spacing after the exchange process has been confirmed in transmission electron microscopy experiments on films prepared from pre- and postexchanged NCs. In addition, the closer interparticle separation in the octylamine-capped NCs is expected to provide better electron conduction through the NC phase, and thus higher charge collection efficiency.

In an effort to improve the photovoltaic performance, we examined the effects of thermal annealing. The results are shown for a representative set of devices, using octylamine-capped NCs with a first-excitonic absorption peak of 1300 nm, in Fig. 2. Annealing at temperatures above ∼160 °C leads to notable changes in I_{sc} and photocurrent under bias. Compared with the unannealed sample, the sample annealed at 220 °C shows an I_{sc} 200 times higher, and a product of $I_{sc} \cdot V_{oc}$ (under 400 mW illumination) about 600 times higher. The short-circuit internal quantum efficiency of the annealed samples is about 0.15%, compared to 0.0064% for the best samples previously reported.[7]
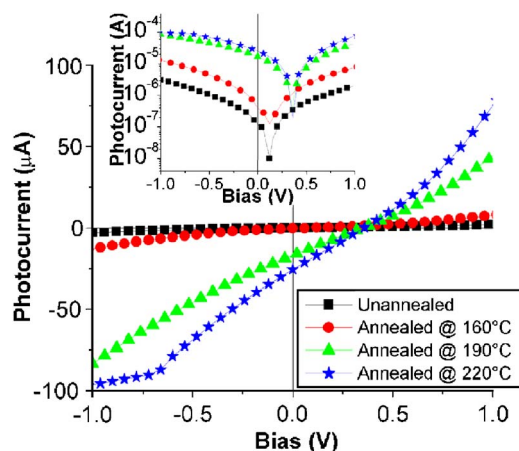
The dependence of the short-circuit current (I_{sc}), open-circuit voltage (V_{oc}), and the fill factor [$(V \cdot I)_{max}/(I_{sc}V_{oc})$] on the incident light power for a device made from a film annealed at 220 °C is shown in Fig. 3. The magnitude of the observed I_{sc} and V_{oc} depends on the incident light intensity. Below 150 mW illumination intensity, I_{sc} increases linearly with power, while at higher intensity I_{sc} depends sublinearly on the light power, which may be ascribed to bimolecular recombination.[1] The power conversion efficiency (maximum electrical output power/incident light power) is about 0.001% at an incident power of 16 mW and decreases with increased power. The low absorbance (<0.06) at the illumination wavelength and the low fill factors are causes of the low-power conversion efficiencies. The low fill factor in our devices could be due to either a high series resistance, possibly due to low carrier mobilities, or a low shunt resistance, possibly from nanoscopic pinholes penentrating the films. Furthermore, the devices likely have a low carrier lifetime/mobility product leading to a strong dependence of the photocurrent on the electric field between 0 V and V_{oc}. If the product of the electric field and the lifetime/mobility were much larger than the active layer thickness, the extraction of photogenerated carriers would depend less on the field; the photocurrent *I-V* curve would then behave closer to the ideal horizontal response in the region between 0 V and V_{oc}, which would correspond to a higher fill factor.
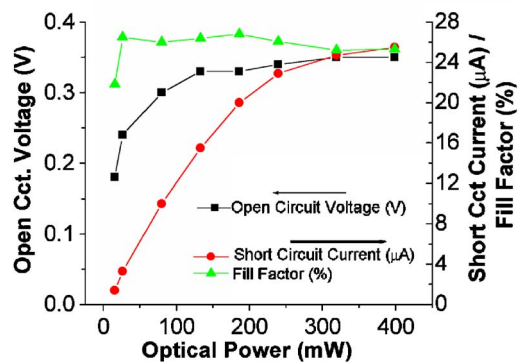

FIG. 3. (Color online) Dependence of the short-circuit current (I_{sc}), open-circuit voltage (V_{oc}), and fill factor [FF=maximum power output/$(I_{sc} * V_{oc})$] on the incident optical power for a device annealed at 220 °C.
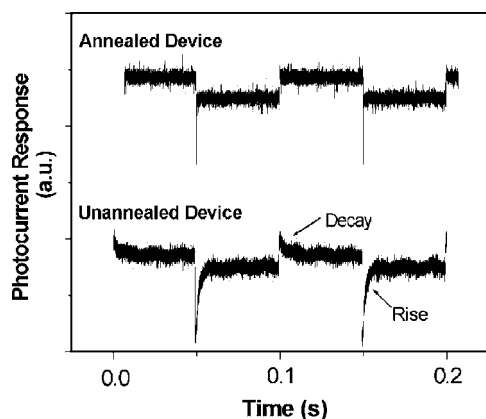
FIG. 4. Temporal behavior of I_{sc} for an unannealed sample (bottom) and a sample annealed at 220 °C (top).

The temporal behavior of I_{sc} for the as-deposited and annealed sample at 220 °C is shown in Fig. 4. Switching the laser off/on or on/off causes an I_{sc} decay to a stable value following a quick rise, or an I_{sc} rise following a quick drop, respectively, for both samples. The annealed sample reaches the stable state much more quickly. The I_{sc} rise time for the unannealed sample is 18 ms, compared to 1.7 ms for the annealed sample. The temporal behavior at zero bias results from charge trapping and release. In the illuminated state, more electrons are trapped at the cathode and more holes at the anode, which screens out the built-in field and diminishes the current. In the dark state, the trapped charges are released and may move in the opposite direction to return to the equilibrium state, as shown by the current spike preceding the settling to the off state.

The improved device performance after annealing is proposed to be due to improved charge separation and improved charge transport. Both the dark and photocurrents were found to increase exponentially with annealing temperature, although the dark current increases at a much lower rate. A 140 times increase in dark current was observed upon annealing at 220 °C, indicating improved charge transport after annealing. Annealing near or above the glass transition temperature (~215 °C) of the polymer could also allow morphology changes in the film that might yield more favorable electrical transport properties in both polymer and NC phases. Such morphology changes could thus yield a more efficient bulk heterojunction structure in the film, improving both charge separation and transport. In addition, we propose that removal of some ligands from the NC surface occurs during annealing, causing: (a) reduced spatial separation of the NC and polymer at the heterojunction interface and thus improved charge separation, and (b) further reduction of the interparticle spacing in the NC phase to improve electron conduction.

We investigated whether heating of the films could result in removal of the ligands from the NC surface. TGA data for an octylamine-capped sample of PbS NCs shows 5% weight loss after heating to 200 °C. In comparison, the oleic acid-capped NCs demonstrated no appreciable weight loss below 300 °C. The TGA data suggest that a certain amount of octylamine ligand is removed from the film during the annealing process at or above 190 °C (the boiling point of octylamine is 175 °C), permitting closer contact between the MEH-PPV backbone chains and the nanocrystal surface, and thus improving the efficiency of the charge transfer at the interface. Complete quenching of the NC photoluminescence after annealing at 220 °C was also observed, suggesting rapid exciton dissociation before recombination, and supporting the conclusion of efficient charge separation between the NC and polymer. The faster time response of the photocurrent in the annealed samples (Fig. 4) is also likely due to the combined effects of the more efficient charge separation and the improved electron transport properties that result after annealing. Further improvement to the efficiency of these devices employing the thermal annealing process may be possible using different ligands, altering the annealing conditions, and selecting conjugated polymers with more favorable hole accepting and/or hole mobility properties to reduce the recombination of charge carriers in the device.

[1]N. C. Greenham, X. Peng, and A. P. Alivisatos, Phys. Rev. B **54**, 17628 (1996).
[2]W. U. Huynh, X. Peng, and A. P. Alivisatos, Adv. Mater. (Weinheim, Ger.) **11**, 923 (1999).
[3]W. U. Huynh, J. J. Dittmer, and A. P. Alivisatos, Science **295**, 2425 (2002).
[4]B. Sun, E. E. Marx, and N. C. Greenham, Nano Lett. **3**, 961 (2003).
[5]W. J. E. Beek, M. M. Wienk, and R. A. J. Janssen, Adv. Mater. (Weinheim, Ger.) **16**, 1009 (2004).
[6]E. H. Sargent, Adv. Mater. (Weinheim, Ger.) **17**, 515 (2005).
[7]S. A. McDonald, G. Konstantatos, S. Zhang, P. W. Cyr, E. J. D. Klem, L. Levina, and E. H. Sargent, Nat. Mater. **4**, 138 (2005).
[8]N. Camaioni, G. Ridolfi, G. Casalbore-Miceli, G. Possamai, and M. Maggini, Adv. Mater. (Weinheim, Ger.) **14**, 1735 (2002).
[9]J. J. Dittmer, R. Lazzaroni, P. Leclère, P. Moretti, M. Granström, K. Petritsch, E. Marseglia, R. H. Friend, J. L. Brédas, H. Rost, and A. B. Holmes, Sol. Energy Mater. Sol. Cells **61**, 53 (2000).
[10]J. J. Dittmer, E. A. Marseglia, and R. H. Friend, Adv. Mater. (Weinheim, Ger.) **12**, 1270 (2000).
[11]W. Feng, A. Fujii, S. Lee, H. Wu, and K. Yoshino, J. Appl. Phys. **88**, 7120 (2000).
[12]W. U. Huynh, J. J. Dittmer, W. C. Libby, G. L. Whiting, and A. P. Alivisatos, Adv. Mater. (Weinheim, Ger.) **13**, 73 (2003).
[13]M. A. Hines and G. D. Scholes, Adv. Mater. (Weinheim, Ger.) **15**, 1844 (2003).
[14]T.-W. F. Chang, A. Maria, P. W. Cyr, V. Sukhovatkin, L. Levina, and E. H. Sargent, Synth. Met. **148**, 257 (2005).